Pergamon

PII: S0042-6989(96)00108-3

Vision Res., Vol. 36, No. 23, pp. 3767–3774, 1996
Copyright © 1996 Elsevier Science Ltd. All rights reserved
Printed in Great Britain
0042-6989/96 $15.00 + 0.00

Flicker Sensitivity as a Function of Spectral Density of External White Temporal Noise

JYRKI ROVAMO,*§ ANTTI RANINEN,† SAKARI LUKKARINEN,† KRISTIAN DONNER‡

Received 8 June 1994; in revised form 22 January 1996

Foveal flicker sensitivity at 0.5–30 Hz was measured as a function of the spectral density of external, white, purely temporal noise for a sharp-edged 2.5 deg circular spot (mean luminance 3.4 log phot td). Sensitivity at any given temporal frequency was constant at low powers of external noise, but then decreased in inverse proportion to the square root of noise spectral density. Without external noise, sensitivity as function of temporal frequency had the well-known band-pass characteristics peaking at about 10 Hz, as previously documented in a large number of studies. In the presence of strong external noise, however, sensitivity was a monotonically decreasing function of temporal frequency. Our data are well described (goodness of fit 90%) by a model comprising (i) low-pass filtering by retinal cones, (ii) high-pass filtering in the subsequent neural pathways, (iii) adding of the temporal equivalent of internal white spatiotemporal noise, and (iv) detection by a temporal matched filter, the efficiency of which decreases approximately as the power −0.58 of temporal frequency. Copyright © 1996 Elsevier Science Ltd

Flicker sensitivity Temporal noise Modelling Human visual system Signal processing

INTRODUCTION

Studies of the human visual system with flickering stimuli have firmly established the general relationship between sensitivity and temporal frequency (Dow, 1907; Ives, 1922; De Lange, 1952; Kelly, 1961; reviewed by Kelly, 1972). At photopic luminance levels, sensitivity to a flickering spot rises with increasing temporal frequency across the low-frequency range, peaks at frequencies around 10 Hz and then declines fairly steeply. Today it is evident that the main properties of this flicker sensitivity function can be accounted for by known physiological transformations in the retina (see Donner & Hemilä, 1996), which can be decomposed into low-pass filtering by photoreceptors (DeVoe, 1962; Fuortes & Hodgkin, 1964; Baylor *et al.*, 1974; Hood & Birch, 1993) and high-pass filtering associated with neural transmission. The low-pass filtering by photoreceptors is in complete agreement with the well-known engineering solution modelling high-frequency attenuation as resulting from a sequence of RC-filters (De Lange, 1952; Matin, 1968; Sperling & Sondhi, 1968; Watson, 1986). For large stimuli (as used here), high-pass filtering is largely due to lateral antagonism (Kelly, 1961, 1969, 1971; Levinson, 1964; Watson, 1986; Donner & Hemilä, 1996).

In the present work we address the nature of the detection process that takes place after these filtering stages. In analogy with a previously published model for spatial vision (Rovamo *et al.*, 1993), we assume that temporal white noise is first added to the signal and detection is thereafter mediated by a temporal matched filter. Although the use of additive noise followed by a temporal matched filter is novel in modelling flicker sensitivity, intrinsic (Burgess *et al.*, 1981) or equivalent (Pelli, 1990) noise combined with the ideal detector for a signal known exactly (Tanner & Birdsall, 1958) has been commonly used in analysing detection and discrimination experiments on spatial and spatiotemporal stimuli in spatiotemporal noise (see e.g. Ahumada & Watson, 1985; Legge *et al.*, 1987; Pelli, 1991).

To test the above model we measured flicker sensitivity at various temporal frequencies in the presence of external, white, purely temporal noise of various magnitudes. We found that the model described the data very well (goodness of fit 90%). An important finding is that the efficiency of detection decreases with increasing temporal frequency.

MODELLING OF FLICKER SENSITIVITY

Photopic visual stimuli varying in time are filtered by the retinal cones and subsequent neural visual pathways

*Department of Optometry and Vision Sciences, University of Wales College of Cardiff, P.O. Box 905, Cardiff CF1 3XF, U.K.
†Institute of Biomedicine, Department of Physiology, P.O. Box 9 (Siltavuorenpenger 20 J), University of Helsinki, FIN-00014 Helsinki, Finland.
‡Department of Biosciences, P.O. Box 17 (Arkadiankatu 7), University of Helsinki, FIN-00014 Helsinki, Finland.
§To whom all correspondence should be addressed [*Email* Rovamo@cardiff.ac.uk].

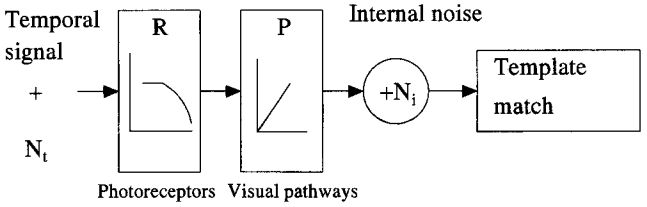

FIGURE 1. Description of the human visual system as a simple temporal signal processing system. First a temporal visual signal + noise (N_t) is low-pass filtered by the modulation transfer function (R) of the photoreceptors of the eye. Then comes high-pass filtering (P) in subsequent neural pathways and addition of internal neural noise (N_i) before signal detection takes place in the brain.

before being interpreted by the human brain. We modelled this complex neurobiological system as a simple signal processing system shown in Fig. 1. First the visual signal and external temporal noise (N_t) are (i) low-pass filtered by the temporal modulation transfer function (R) of the cone photoreceptors in the human retina. This is followed by (ii) high-pass filtering with the temporal modulation transfer function (P) of the neural visual pathways resulting mainly from lateral inhibition and (iii) subsequent addition of internal neural noise (N_i), before (iv) signal detection takes place in the brain. Detection is mediated by a temporal matched filter (see e.g. Hauske *et al.*, 1976). It is an ideal detector, because in white noise a matched filter produces the best possible signal-to-noise ratio (Tanner & Birdsall, 1958).

Flicker sensitivity as a function of temporal frequency

After being filtered by the modulation transfer functions (see Fig. 1) of cones (R) and visual pathways (P), the contrast energies of the flicker signal at threshold are

$$E'_{\text{human}}(f) = R^2(f)P^2(f)c^2_{\text{rms}}t \quad (1)$$

and

$$E'_{\text{ideal}}(f) = d'^2N'(f) \quad (2)$$

for the human and ideal detection filters, respectively. In equation (1) f is temporal frequency, t is exposure time, c_{rms} is the experimentally measured rms contrast of a sinusoidal flicker signal [see equation (10)] at threshold, and $c^2_{\text{rms}}\ t$ is the corresponding external contrast energy integrated across time. Equation (1) is only approximate in the sense that it assumes that all the contrast energy of the flickering signal is on its nominal temporal frequency. In equation (2), d' is the detectability index (Tanner & Birdsall, 1958) referring to the signal-to-noise ratio at a detection filter and N' is the spectral density of the total noise in the visual system:

$$N'(f) = R^2(f)P^2(f)N_t + N_{it}(f). \quad (3)$$

According to equation (3) external temporal noise N_t is first filtered by the temporal modulation transfer functions of the retinal cones and subsequent neural visual pathways before the temporal equivalent of internal neural noise N_{it} is added (see Fig. 1). For the sake of simplicity, N_{it} is assumed to be white (i.e., $N_{it}(f) = N_{it}$), which means that its spectral density is constant across the temporal frequency spectrum. Equation (3) also assumes that flickering stimuli are viewed in bright light so that quantal noise is negligible. For the effect of quantal noise in spatial vision see Rovamo *et al.* (1994). Equations (1)–(3) are general in the sense that they are true for any version of the model shown in Fig. 1. Our threshold estimation algorithm gives estimates at the probability level of 0.84 for correct responses in a two-alternative forced-choice task. From Elliot's (1964) forced-choice tables, the value of d' is thus 1.4.

Let the critical spectral density (N_c) of external temporal noise transferred through the cones and visual pathways be equal to N_{it} at all temporal frequencies. This means that N_{tc} represents the external temporal equivalent of internal, white, neural noise. Conversely, if the temporal equivalent of internal neural noise could be back-projected into the visual field, it would equal the critical noise. Thus,

$$N_{ct} = N_{it}/[R^2(f)P^2(f)]. \quad (4)$$

The efficiency (Tanner & Birdsall, 1958) of the human detection filter is

$$\eta = E'_{\text{ideal}}(f)/E'_{\text{human}}(f). \quad (5)$$

By combining equations (1)–(5) we can solve rms flicker sensitivity (S) as the inverse of c_{rms}:

$$S(f) = \sqrt{t\eta(f)}/\{d'\sqrt{N_{tc}(f)}[1 + N_t/N_{tc}(f)]^{0.5}\}. \quad (6)$$

Equation (6) means that at the low spectral densities of external noise rms flicker sensitivity is constant, whereas at the high spectral densities sensitivity decreases in inverse proportion to the square root of the increasing spectral density of noise. The critical spectral density (N_{tc}) of noise marks the transition between the constant and decreasing parts of equation (6). Equation (6) also gives the maximum sensitivity (S_{max}) obtainable without external temporal noise ($N_t = 0$) at the exposure duration and stimulus size used.

The modulation transfer function of the cone photoreceptors as a function of temporal frequency

The impulse response of the foveal cone photoreceptors has been modelled by the Poisson variant of a class of linear filter cascade models (Baylor *et al.*, 1974). Such models successfully describe photoreceptor responses to flashes and steps of light in the retinas of a wide variety of species, including cone responses in turtles and primates (Schnapf *et al.*, 1990; Hood & Birch, 1993; Schneeweis & Schnapf, 1995).

The temporal modulation transfer function of cones according to the Poisson formulation is

$$R = R(0)[1 + (2\pi f\tau)^2]^{-n/2}. \quad (7)$$

where $R(0)$ is its zero frequency asymptote (cf. Baylor *et al.*, 1979, 1980). For the sake of simplicity $R(0)$ is assumed to be equal to unity. The parameter n is an

integer corresponding to the number of stages in the filter cascade and it determines the waveform. Baylor *et al.* (1974) obtained good fits to turtle cone responses with $n = 6$ or 7. Hood & Birch (1993) found that $n = 6$ provided the best description for the a-wave in the cone ERG response of the human eye. We therefore used the value $n = 6$. The time constant τ defines the overall time scale. The inverse of expression $2\pi\tau$ in equation (7) can be replaced by f_c. It is the temporal cut-off frequency at which R has decreased to 0.167 when $n = 6$.

METHODS

Apparatus

Flickering spots were generated under computer control (ALR Business Veisa 486/33 MHz) on a 16 in. RGB multiscan monitor (Eizo Flexscan 9080i with fast phosphor B22) driven at the frame rate of 60 Hz by a graphics board (Orchid's ProDesigner VGA+) that generated 640×480 pixels. The pixel size was 0.42×0.42 mm^2.

The display was used in a white mode. Its CIE (1931) (x,y) chromaticity coordinates, measured with a Bentham PMC 3B Spectroradiometer, were (0.30, 0.31). The average luminance of the display was measured with a Minolta Luminance Meter LS-110. It was set to 50 phot cd/m^2, corresponding to 130 scot cd/m^2, measured with the Spectroradiometer. The non-linear luminance response of the screen was linearized by using its inverse function when computing the temporal luminance modulation waveform.

To obtain a monochrome palette of 16,384 (14 bits) intensity levels and a monochrome signal of 256 intensity levels (8 bits) from the palette we combined the red, green, and blue outputs of the VGA board by using a video summation device built according to Pelli & Zhang (1991). The range of 14 bits allowed the measurement of sensitivity with flicker signals consisting of about 20 different grey levels even when Michelson contrast was as low as 0.002. The amplitudes and frequencies of flickering stimuli were checked with a phototransistor TIL81 (Texas Instruments). There was no attenuation of amplitude even at 30 Hz, which was the highest temporal frequency used.

Stimuli

Sinusoidal flicker with or without white temporal noise was used. The diameter of the circular flicker field with a sharp edge was 10 cm. The equiluminous surround was limited to a circular area of 20 cm in diameter by black cardboard. The viewing distance was 228 cm.

The temporal luminance waveform of the sinusoidally flickering stimulus was

$$L(t) = L_0[1 + m\cos(2\pi ft + \Phi)], \tag{8}$$

where L_0 is the average luminance of the screen, m is the modulation depth of flicker, f is flicker frequency in Hz, t is time in sec, and Φ is phase angle. At 0.5–20 Hz, phase angle was 90 deg. However, at 30 Hz it was 0 deg, because the frame rate of our display was only 60 Hz. Thus, temporal modulation at 30 Hz was in fact a square-wave flicker, because only luminance maxima and minima were shown.

Before each trial the temporal luminance waveform of the flickering stimulus for the whole exposure duration of 2 sec was calculated by means of a software developed by Risto Näsänen. It was written in Basic language and translated by a Microsoft Professional Basic 7.0 compiler. The software utilized the graphics subroutine library of a Professional Halo 2.0 developed by Media Cybernetics. The temporal waveform was produced by changing the colour look-up table of the graphics board during each vertical retrace period of the display within the exposure duration.

White, purely temporal noise was produced by adding to the stimulus at each time pixel (frame) a random number drawn independently from a Gaussian luminance distribution with zero mean and truncation at ± 2.5 SD-units. The rms contrast of temporal noise was varied by changing the standard deviation of the Gaussian luminance distribution. Successive temporal noise pixel luminances were uncorrelated. Thus, the one-dimensional temporal noise produced was white up to a cut-off frequency determined by the frame rate of our display.

Contrast energies of flickering stimuli without noise were calculated by numerical integration across time as

$$E = \sum c^2(t)\Delta t, \tag{9}$$

where $c(t) = [L(t) - L_0]/L_0$, Δt is the duration of each temporal pixel, i.e., one frame in seconds, $L(t)$ is the temporal luminance waveform from equation (8), and L_0 is the average luminance of the screen. Thus, for each temporal pixel the deviation of luminance from the average luminance was first divided by the average luminance to obtain a measure of local contrast in time. These measures were then squared and multiplied by temporal pixel duration. Their sum then indicates the contrast energy. Rms contrast was thereafter calculated as

$$c_{\mathrm{rms}} = \sqrt{(E/t)}, \tag{10}$$

where t is stimulus exposure duration in seconds. Rms contrast is thus equal to the standard deviation of the luminance distribution calculated frame by frame across the stimulus duration and divided by the average luminance. For sinusoidal flicker rms contrast is approximately equal to Michelson contrast divided by $\sqrt{2}$. Michelson contrast is calculated as $(L_{\max} - L_{\min})/(L_{\max} + L_{\min})$, where $L_{\max}$ and $L_{\min}$ are the maximum and minimum luminances of the temporal sinusoidal flicker.

For the temporal frequencies where temporal noise is white the spectral density of noise was calculated (Legge *et al.*, 1987) as

$$N_e = c_n^2\Delta t, \tag{11}$$

where c_n is the rms contrast of noise calculated by dividing the standard deviation of the Gaussian luminance distribution of noise by the average luminance and Δt is the temporal pixel duration in seconds. In our experiments c_n varied between 0 and 0.3.

Procedures

Experiments were performed in a dark room, the only light source being the display. The stimuli were viewed monocularly. To control retinal illuminance the pupil was dilated to 8 mm with 1–4 drops of 10% phenylepherine (metaoxedrine) hydrochloride (Smith & Nephew Pharmaceuticals Ltd., Romford, England). Metaoxedrine leaves accommodation unaffected. The other eye was covered with a black eye pad.

The average retinal illuminance produced by our display through a pupil with 8 mm diameter was about 2,500 phot td, corresponding to 6500 scot td. The centre of the stimulus field was fixated during the experiment. A black spot served as a fixation mark. The subject's head was stabilized by a chin rest.

Flicker sensitivity is the inverse of rms contrast at threshold. The contrast thresholds were determined by a two-alternative forced-choice algorithm with four-correct-then-down/one-wrong-then-up rule. For further details see Mustonen *et al.* (1993). Each trial consisted of two 2 sec exposures, separated by 0.6 sec. Both exposures were accompanied by a sound signal. One exposure contained only temporal noise while the other one contained both the signal and a different sample of temporal noise. Between the two exposures and during the inter-trial interval the subject saw only the blank equiluminous field. The subject indicated which of the two exposures contained the flicker signal by pressing one of two keys on a computer keyboard. A response was followed by a sound signal that was different depending on whether the response was correct or incorrect, thus providing feedback to the subject. A new trial began 250 msec after the observer's response.

The threshold contrast required that the probability of 0.84 correct was obtained as the arithmetic mean of the last eight reversal contrasts (Wetherill & Levitt, 1965). Every data point shown is the geometric mean of at least three thresholds measurements.

Subjects

Two experienced subjects, aged 24 and 44 years, served as observers. A.R. was an uncorrected hyperope (+1.00 D oa). S.L. was an emmetrope. Their accommodation had a range of at least 2 D. Hence, both subjects were emmetropes at the viewing distance of 228 cm used in our experiments. With the optimal refraction the monocular visual acuity with Sloan letters at 4 m was 1.2 for the left eye of A.R. and for the right eye of S.L.

RESULTS

Figure 2 shows rms flicker sensitivities (S) measured at eight different temporal frequencies as functions of the spectral density (N_t) of external noise. Sensitivity was first constant, but then started to decrease with increasing noise spectral density. The slope of the decrease in double logarithmic coordinates reached about -0.5 at high noise powers. The critical spectral density of noise (N_{tc}), marking the beginning of the decreasing region,

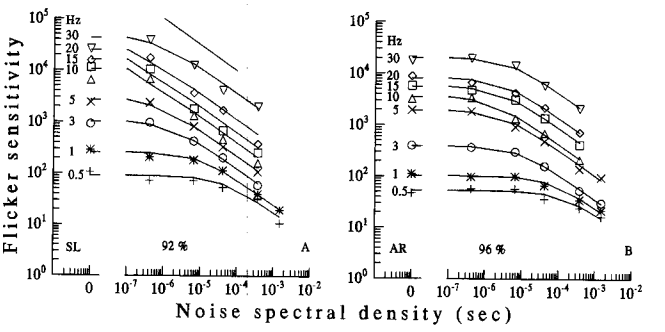

FIGURE 2. Foveal rms flicker sensitivity as a function of the spectral density of external noise within 0 and 1.5×10^{-3} sec at 0.5–30 Hz. Smooth curves, calculated by equation (6), are the least squares curves fitted to the data. Goodness of fit is indicated as percentages. For clarity of presentation the curves and data points have been shifted vertically. In both frames the lowest curve and data are in their correct place but higher flicker rates have been shifted upwards by factors 2, 4, 8, 16, 32, 64, and 256 for S.L. and by factors 2, 4, 11, 19, 42, 70, and 256 for A.R., respectively. The diameter of the circular, sinusoidally flickering spot was 2.5 deg. The diameter of the equiluminous surround was 5 deg. Subjects are as indicated. The short solid line in A shows the slope of -0.5.

varies with temporal frequency. Note, for example, that for a noise spectral density of 10^{-6} s, the slopes of the sensitivity curves become steeper as frequency increases until exceeding 15 Hz. Above 15 Hz the slopes again become more shallow. This suggests that N_{tc} has a minimum value in the range of 10–15 Hz, since the lower the external noise level at which the slope reaches -0.5, the smaller the value of N_{tc}.

The smooth curves were calculated according to equation (6) fitted separately to the flicker sensitivity data measured for each temporal frequency and subject. The goodness of fit calculated across the temporal frequencies by equation (A6) (Appendix) was 92–96% for the data of two subjects. The fitting yielded estimates of N_{tc}, which have been plotted as a function of temporal frequency in Fig. 3(A).

As expected, N_{tc} first decreased with increasing flicker frequency reaching a minimum at 10–15 Hz and increased thereafter. The estimates of N_{tc} were about six times greater for subject A.R. than S.L. at all temporal frequencies. Thus, the dependence of N_{tc} on temporal frequency was similar for both subjects. The smooth curves of Fig. 3(A) and (B) will be explained further below.

In Fig. 3(B) the estimates of N_{tc} raised to an exponent of -0.5 are plotted as a function of temporal frequency. To understand the implications of this presentation, the reader should consider equation (4) according to which the dependence of $N_{tc}^{-0.5}$ on temporal frequency should reproduce the shape of the temporal modulation transfer function of the human visual system under the assumption that the intrinsic noise is white, i.e., N_{it} is constant across temporal frequencies. As Fig. 3(B) shows, $N_{tc}^{-0.5}$ first increased with flicker frequency reaching a maximum at 10–15 Hz and decreased thereafter.

In the view of the purely low-pass modulation transfer

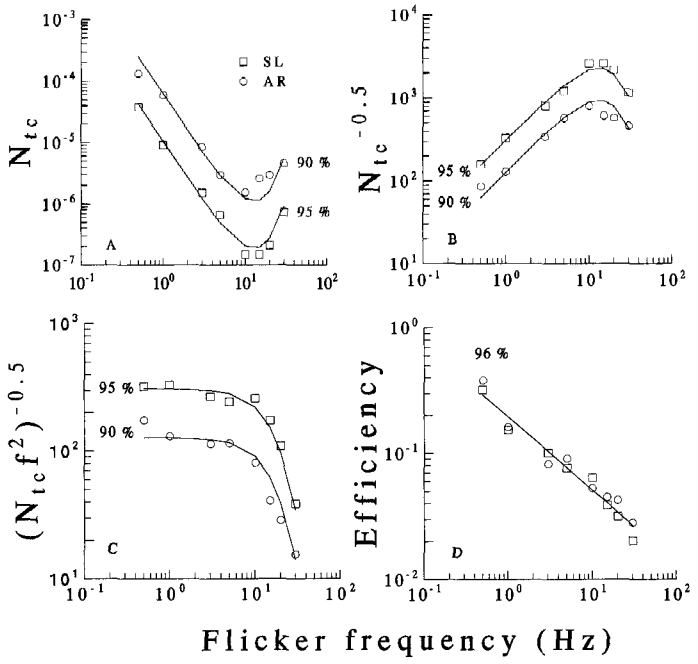

FIGURE 3. (A) The estimates of the critical spectral density (N_{tc}) of temporal noise plotted as a function of temporal frequency. (B) The estimates of $N_{tc}^{-0.5}$ plotted as a function of temporal frequency. (C) The estimates of $(N_{tc}f^2)^{-0.5}$ plotted as a function of temporal frequency. The smooth curves in (A–C) are calculated by equation (4). (D) The estimates of efficiency plotted as a function of temporal frequency. In (A–D) percentages refer to the goodness of fit and subjects were as indicated in (A).

function of cones (R), the increase of $N_{tc}^{-0.5}$ as a function of temporal frequency (f) in Fig. 3(B) reflects neural high-pass filtering (P). The increase in double logarithmic coordinates was linear with a slope of 1. This implies that the modulation transfer function of the neural visual pathways is proportional to temporal frequency. For the sake of simplicity we now assume that, in analogy with our previously published model of spatial vision (Rovamo *et al.*, 1993),

$$P(f) = f. \tag{12}$$

In Fig. 3(C) the estimates of $[N_{it}^{-0.5}\, R(f)]$, calculated according to equation (4) as $(N_{tc}f^2)^{-0.5}$, were plotted in double logarithmic coordinates as a function of temporal frequency. The shape of this function is thus expected to reproduce that of $R(f)$, the modulation transfer function of retinal cones. As Fig. 3(C) shows, $(N_{tc}f^2)^{-0.5}$ was first constant but then started to decrease with increasing flicker frequency.

The low-pass attenuation due to cone photoreceptors as a function of flicker frequency was modelled by equation (7) with $n = 6$. Hence, equation (3a) was fitted to the average data of the subjects from Fig. 3(C), because the dependence of $(N_{tc}f^2)^{-0.5}$ on temporal frequency was similar for both subjects. The values of f_c and τ were found to be 29.0 Hz, and 5.49 msec, respectively. The best fit of the template to the individual data was obtained* when $N_{it} = 1.05 \times 10^{-5}$ sec for S.L. and 6.20×10^{-5} sec for A.R. The smooth curves in Fig. 3(A–C) were calculated by means of equations (4), (7) and (12). Goodness of fit, calculated by equation (A6), was 90–95% for the data of two subjects.

Figure 3(D) gives [cf. equation (5)] the estimates of detection efficiency $\eta = d'^2 N_{tc}(f)/(S_{max}^{-2}\, t)$ as a function of flicker frequency on double logarithmic coordinates. Log η decreased linearly with log f. Efficiency was 0.3–0.4 at 0.5 Hz and decreased to 0.02–0.03 at 30 Hz. The equation of the regression line in a non-logarithmic form is

$$\eta = 0.196 f^{-0.581}, \tag{13}$$

producing the goodness of fit of 96%.

In Fig. 4 the rms flicker sensitivity data of Fig. 2 have been replotted as a function of temporal frequency in double logarithmic coordinates. Smooth curves were calculated by equations (6), (7), (12), and (13).

In agreement with a large number of earlier studies (reviewed by Kelly, 1972), flicker sensitivity without external noise first increased with temporal frequency reaching a maximum at about 10 Hz and decreased thereafter. At strong external noise flicker sensitivity decreased monotonically with increasing temporal frequency. Examination of Fig. 4 revealed that without external noise, flicker sensitivity was at all temporal frequencies better for subject S.L. than A.R. but similar for both subjects in strong noise. Equation (6) described the flicker sensitivity data of Fig. 4 very well. The goodness of fit, calculated by equation (A6), was 90%. In equation (6) the only difference between the subjects was the spectral density of the temporal equivalent of internal neural noise, which was six times higher for A.R. than S.L.

*The estimates of $(N_{tc}f^2)^{-0.5}$ for each subject were first divided by $R(f)$ and then geometrically averaged across the temporal frequencies studied in order to get an estimate of $N_{it}^{-0.5}$ for each subject.

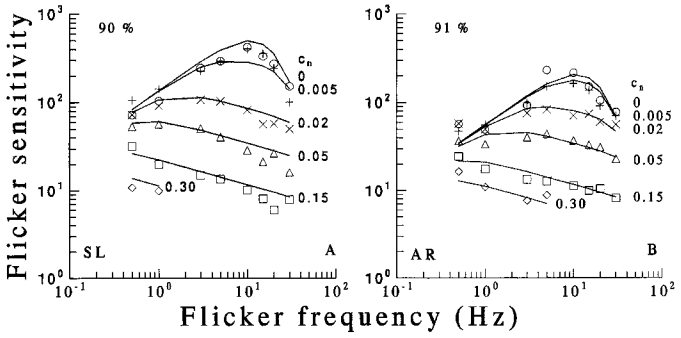

FIGURE 4. Rms flicker sensitivity data from Fig. 2 replotted as a function of temporal frequency. Smooth curves were calculated by equation (6). The rms contrasts of temporal noise are shown in the vicinity of the curves. Percentages refer to the goodness of fit.

DISCUSSION

Noise-limited detection and the temporal matched filter

Noise-limited detection. The goodness of fit of our model to the flicker sensitivity data, measured at the temporal frequencies of 0.5–30 Hz and noise spectral densities of $0–1.5 \times 10^{-3}$ sec, was 90%. Flicker sensitivity measured at a fixed temporal frequency was first independent of the magnitude of external noise, but then decreased in inverse proportion to the square root of external noise spectral density. The dependence of flicker sensitivity on external noise is analogous to that of grating contrast sensitivity on the spectral density of external noise (Pelli, 1990; Rovamo *et al.*, 1992). On the other hand, the critical spectral density of external temporal noise (N_{tc}) decreased in inverse proportion to temporal frequency squared in the range 0.5–10 Hz and increased thereafter. This is analogous to the finding that the critical spectral density of spatial noise is inversely proportional to spatial frequency squared at low and medium frequencies (Rovamo *et al.*, 1992).

Under the assumptions that (i) the zero frequency asymptote $R(0)$ of the modulation transfer function of retinal cones is equal to unity, (ii) internal neural noise is white, and (iii) the modulation transfer function of the subsequent neural visual pathways is equal to temporal frequency, the temporal equivalent of the spectral density of internal, spatiotemporal, white noise was found to be 1.05×10^{-5} sec for S.L. and 6.20×10^{-5} sec for A.R. at all temporal frequencies. As S.L. was 24 and A.R. 44 years old, the difference might reflect an age-dependent increase in the magnitude of internal noise. It could be one reason for the decrease of flicker sensitivity with advancing age (Kim & Mayer, 1994).

Provided that internal neural noise is white, the effectiveness of external temporal noise in reducing flicker sensitivity at any given temporal frequency will directly reveal how well that frequency passes through the total temporal modulation transfer function of the human visual system. We think this is why the band-pass shaped frequency dependence of $N_{tc}^{-0.5}$ reflected the complete temporal modulation transfer function of the human visual system.

Matched-filter detector. When detection is limited by external white noise i.e., $N_t \gg N_{it}$, flicker sensitivity with a matched filter of constant efficiency is expected to be independent of temporal frequency [cf. equation (5)]. This is due to the fact that at all temporal frequencies both the signal and external noise are attenuated equally by the filtering stages. The relatively flat frequency dependence of flicker sensitivity in strong external noise (see Fig. 4) is basically consistent with this. In contrast, a peak-to-trough detector acting on signal amplitude would always, with or without noise, roughly reproduce the bandpass shape of the modulation transfer function (Graham & Hood, 1992; Von Wiegand *et al.*, 1995). It is also worth noting that although without added noise A.R. had significantly lower sensitivity than S.L. at all temporal frequencies, the sensitivities of the two subjects became similar at high levels of external noise.

Nevertheless, in strong external noise flicker sensitivity was not constant, but decreased slowly with increasing temporal frequency. According to our model this implies that the efficiency of detection decreased, suggesting that the temporal sampling window of the matched filter might have contracted with increasing temporal frequency. In analogy with spatial vision (Rovamo *et al.*, 1993), this contraction might be due to the increase of the number of cycles in the stimulus with constant duration of 2 sec. Changes of sampling window size in time as well as other factors that may produce the efficiencies observed merit further study. The important general conclusion at this stage is that the efficiency of the detector depends on the stimulus parameters.

The temporal modulation transfer function

Cone kinetics and R. Without external noise, the dependency of flicker sensitivity on temporal frequency exhibited the general shape previously found in a large number of studies (reviewed by Kelly, 1972). We modelled the decrease at high frequencies by a physiologically realistic modulation transfer function of retinal cones (R). The cut-off frequency of R was found to be 29 Hz, corresponding to a time constant of 5.5 msec. Hood & Birch (1993), when fitting the a-wave of

the human cone ERG with the same model, obtained $\tau = 6.8$ msec at the adapting luminance 0.9 log td. The acceleration of the photoreceptor response with increasing mean luminance would then lead us to expect $\tau = 3$–4 msec in our experiments at 3.4 log td (Donner *et al.*, 1995; cf. Roufs, 1972). Given the limited frequency range of our measurements ($\leqslant 30$ Hz) and the uncertainties involved in comparing results obtained at various mean luminances, the agreement in the absolute time scale of cone responses is reasonable.

Our model would overestimate sensitivities at very high frequencies and for example, the critical flicker fusion frequency (CFF). There are several possible explanations for this: (i) the modulation transfer function of the cones falls more steeply above 30 Hz, (ii) the modulation transfer function of the neural pathways no longer grows above 30 Hz; (iii) the decrease of detection efficiency becomes steeper above 30 Hz.

The neural modulation transfer function P. The critical spectral density of external noise decreased with a slope of -2 in double logarithmic coordinates across the range of 0.5–10 Hz. On the basis of equations (4) and (7), this indicates that the modulation transfer function (P) of the neural visual pathways is proportional to temporal frequency f. There are good reasons to believe that for extended stimuli P is largely shaped by lateral antagonism (Kelly, 1961, 1969). Indeed, a very accurate proportionality between P and f is produced by the phase-lagging, subtractive surround signal in the difference-of-Gaussian receptive fields of retinal ganglion cells (Donner & Hemilä, 1996: cf. Enroth-Cugell *et al.*, 1983). Ganglion cell data provide no support for the easy solution of tailoring the high-frequency attenuation of the antagonistic input to fit the experimental data (Burbeck & Kelly, 1980; Watson, 1986) since the antagonistic surround in fact transmits high frequencies as well as or better than the receptive field centre (Frishman *et al.*, 1987). Admittedly, the potentiation of lateral antagonism seen with very large fields (Kelly, 1959) is likely to include post-retinal components. On the other hand, P as isolated here may include some additional effects, such as high-pass filtering even in the centre pathway of the receptive field (Baylor & Fettiplace, 1977; Lankheet *et al.*, 1989) and/or some low-frequency attenuation originating in the cones themselves (see Baylor & Hodgkin, 1974; Schnapf *et al.*, 1990).

SUMMARY

Our model of flicker sensitivity uses a modulation transfer function based on the well-known n-stage low-pass filter of retinal photoreceptors combined with high-pass filtering by the neural visual pathways with transfer proportional to temporal frequency. Signal detection against white intrinsic noise is assumed to be mediated by a temporal matched filter. The efficiency of the matched filter was found to decrease with increasing temporal frequency. The use of (i) intrinsic noise and (ii) a matched filter as the detector is a clear advance in comparison to models based on classical peak-to-trough detectors. Under the latter type models, flicker sensitivity as a function of temporal frequency will even under dominant external noise reproduce the composite modulation function of the preceding stages, in conflict with our results.

REFERENCES

Ahumada, A. J. Jr & Watson, A. B. (1985). Equivalent-noise model for contrast detection and discrimination. *Journal of the Optical Society of America A, 2*, 1133–1139.

Baylor, D. A. & Fettiplace, R. (1977). Transmission from photoreceptors to ganglion cells in turtle retina. *Journal of Physiology, London, 271*, 391–424.

Baylor, D. A. & Hodgkin, A. L. (1974). Changes in time scale and sensitivity in turtle photoreceptors. *Journal of Physiology, 242*, 729–758.

Baylor, D. A., Hodgkin, A. L. & Lamb, T. D. (1974). The electrical response of turtle cones to flashes and steps of light. *Journal of Physiology, London, 242*, 685–727.

Baylor, D. A., Lamb, T. D. & Yau, K.-W. (1979). Responses of retinal rods to single photons. *Journal of Physiology, London, 288*, 613–634.

Baylor, D. A., Matthews, G. & Yau, K.-W. (1980). Two components of electrical dark noise in toad retinal rod outer segments. *Journal of Physiology, London, 309*, 591–621.

Burbeck, C. A. & Kelly, D. H. (1980). Spatiotemporal characteristics of visual mechanisms. Excitatory–inhibitory model. *Journal of the Optical Society of America, 70*, 1121–1126.

Burgess, A. E., Wagner, R. F., Jennings, R. F. & Barlow, H. B. (1981). Efficiency of human visual signal discrimination. *Science, 214*, 93–94.

De Lange, H. (1952). Experiments on flicker and some calculations on an electric analogue of the foveal systems. *Physica, 18*, 935–950.

DeVoe, R. D. (1962). Linear superposition of retinal action potentials to predict electrical flicker responses from the eye of the wolf spider, *Lycosa baltimoriana* (Keyserling). *Journal of General Physiology, 46*, 75–96.

Donner, K. & Hemilä, S. (1996). Modelling the spatiotemporal modulation response of ganglion cells with difference- of-gaussians receptive fields: Relation to photoreceptor response kinetics. *Visual Neuroscience, 13*, 173–186.

Donner, K., Koskelainen, A., Djupsund, K. & Hemilä, S. (1995). Changes in retinal time scale with light-adaptation: Observations on rods and ganglion cells in frog retina. *Vision Research, 35*, 2255–2266.

Dow, J. S. (1907). The speed of flicker photometers. *Electrician, 59*, 255–257.

Elliot, P. (1964). Forced choice tables (Appendix 1). In Swets, J. A. (Ed.), *Signal detection and recognition by human observers* (pp. 679–684). New York: Wiley.

Enroth-Cugell, C., Robson, J. G., Schwietzer-Tong, D. E. & Watson, A. B. (1983). Spatio-temporal interactions in cat retinal ganglion cells showing linear spatial summation. *Journal of Physiology, London, 341*, 279–307.

Frishman, L. J., Freeman, A. W., Troy, J. B., Schweitzer-Tong, D. E. & Enroth-Cugell, C. (1987). Spatiotemporal frequency responses of cat retinal ganglion cells. *Journal of General Physiology, 89*, 599–628.

Fuortes, M. G. F. & Hodgkin, A. L. (1964). Changes in time scale and sensitivity in the ommatidia of Limulus. *Journal of Physiology, London, 172*, 239–263.

Graham, N. & Hood, D. C. (1992). Quantal noise and decision rules in dynamic models of light adaptation. *Vision Research, 32*, 779–787.

Hauske, G., Wolf, W. & Lupp, U. (1976). Matched filters in human vision. *Biological Cybernetics, 22*, 181–188.

Hood, D. C. & Birch, D. G. (1993). Human cone receptor activity: The leading edge of the a-wave and models of receptor activity. *Visual Neuroscience, 10*, 857–871.

Ives, H. (1922). A theory of intermittent vision. *Journal of the Optical Society of America and Review of Scientific Instruments, 6*, 343–361.

Kelly, D. H. (1959). Effects of sharp edges in a flickering field. *Journal of the Optical Society of America, 49*, 730–732.
Kelly, D. H. (1961). Visual responses to time-dependent stimuli. I. Amplitude sensitivity measurements. *Journal of the Optical Society of America, 51*, 422–429.
Kelly, D. H. (1969). Diffusion model of linear flicker responses. *Journal of the Optical Society of America, 59*, 1665–1670.
Kelly, D. H. (1971). Theory of flicker and transient responses, I. Uniform fields. *Journal of the Optical Society of America, 61*, 537–546.
Kelly, D. H. (1972). Flicker. In Jameson, D. & Hurvich, L. M. (Eds), *Handbook of sensory physiology. Volume VII/4, Visual psychophysics* (pp. 271–302). Berlin: Springer.
Kim, C. B. Y. & Mayer, M. J. (1994). Foveal flicker sensitivity in healthy ageing eyes. II. Cross-sectional ageing trends from 18 through 77 years of age. *Journal of the Optical Society of America A, 11*, 1958–1969.
Lankheet, M. J. M., Molenaar, J. & van de Grind, W. A. (1989). Frequency transfer properties of the spike generating mechanism of cat retinal ganglion cells. *Vision Research, 29*, 1649–1661.
Legge, G. E., Kersten, D. & Burgess, A. (1987). Contrast discrimination in noise. *Journal of the Optical Society of America A, 4*, 391–404.
Levinson, J. (1964). Nonlinear and spatial effects in the perception of flicker. *Documenta Ophthalmologica, 10*, 36–55.
Mäkelä, P., Whitaker, D. & Rovamo, J. (1993). Modelling of orientation discrimination across the visual field. *Vision Research, 33*, 723–730.
Matin, L. (1968). Critical duration, the differential luminance threshold, critical flicker frequency, and visual adaptation: A theoretical treatment. *Journal of the Optical Society of America, 58*, 404–415.
Mustonen, J., Rovamo, J. & Näsänen, R. (1993). The effects of grating area and spatial frequency on contrast sensitivity as a function of light level. *Vision Research, 33*, 2065–2072.
Pelli, D. G. (1990). The quantum efficiency of vision. In Blakemore, C. (Ed.), *Coding and efficiency* (pp. 3–24). Cambridge: Cambridge University Press.
Pelli, D. G. (1991). Noise in the visual system may be early. In Landy, M. S. & Movshon, J. A. (Eds), *Computational models of visual processing* (pp. 147–151). Cambridge: Cambridge University Press.
Pelli, D. G. & Zhang, L. (1991). Accurate control of contrast on microcomputer displays. *Vision Research, 31*, 1337–1350.
Roufs, J. A. J. (1972). Dynamic properties of vision—I. Experimental relationships between flicker and flash thresholds. *Vision Research, 32*, 261–276.
Rovamo, J., Luntinen, O. & Näsänen, R. (1992). Contrast sensitivity and efficiency of grating area and spectral density of spatial noise. *OSA Technical Digest Series, 23*, 93.
Rovamo, J., Luntinen, O. & Näsänen, R. (1993). Modelling the dependence of contrast sensitivity on grating area and spatial frequency. *Vision Research, 33*, 2773–2788.
Rovamo, J., Mustonen, J. & Näsänen, R. (1994). Modelling contrast sensitivity as a function of retinal illuminance and grating area. *Vision Research, 34*, 1301–1314.
Schnapf, J. L., Nunn, B. J., Meister, M. & Baylor, D. A. (1990). Visual transduction in cones of the monkey *Macaca fascularis*. *Journal of Physiology, London, 427*, 681–713.
Schneeweis, D. M. & Schnapf, J. L. (1995). Photovoltage of rods and cones in the macaque retina. *Science, 268*, 1053–1055.
Sperling, G. & Sondhi, M. M. (1968). Model for visual luminance discrimination and flicker detection. *Journal of the Optical Society of America, 58*, 1133–1145.
Tanner, W. P. & Birdsall, T. G. (1958). Definitions of d' and η as psychophysical measures. *Journal of the Acoustical Society of America, 30*, 922–928.
von Wiegand, E., Hood, D. C. & Graham, N. (1995). Testing a computational model of light-adaptation dynamics. *Vision Research, 35*, 3037–3051.
Watson, A. B. (1986). Temporal sensitivity. In Boff, K. R., Kaufman, L. & Thomas, J. P. (Eds), *Handbook of perception and human performance, Volume I.* New York: Wiley-Interscience.
Wetherill, G. B. & Levitt, H. (1965). Sequential estimation of points on a psychometric function. *British Journal of Mathematical and Statistical Psychology, 18*, 1–10.

Acknowledgements—We thank the Academy of Finland, Ministry of Education, the Association of Finnish Ophthalmic Opticians, Information Centre of Optics Business, and the Optics Division of Instrumentarium Corporation for support. Antti Raninen was supported by grants from the Finnish Cultural Foundation and Oskar Öflund Foundation. We also thank Dr. Risto Näsänen for writing the software used in the experiments.

APPENDIX

The Least Squares Curves

Flicker sensitivity as a function of the spectral density of external temporal noise was modelled by fitting equation (6) to the experimental data at each temporal frequency and subject separately. This was obtained by finding the minimum of the following:

$$G = \sum_{j=1}^{n} [\{S_j^{-2}(f) - k_1(f) - k_2(f)N_{tj}\}/S_j^{-2}(f)]^2 \qquad \text{(A1)}$$

where $k_1(f) = S_{max}{}^{-2}(f)$, $k_2(f) = S_{max}{}^{-2}(f)N_c^{-1}(f)$, and $S_j(f)$ are flicker sensitivities corresponding to spectral densities N_{tj} in Fig. 2. Equation (1a) was transformed to

$$G = \sum_{j=1}^{n} (1 - k_1 x_{1j} - k_2 x_{2j})^2, \qquad \text{(A2)}$$

where $x_{1j} = S_j^2$, $x_{2j} = S_j^2 N_{tj}$. The values of k_1 and k_2 that minimize G were then found by the method described in Mäkelä *et al.* (1993). Thereafter we calculated $S_{max}(f) = k_1^{-0.5}(f)$, $N_{tc}(f) = k_1(f)/k_2(f)$.

Low-pass attenuation due to retinal receptors as a function of temporal frequency was modelled by equation (7). Hence, equation

$$Q(f) = N_{it}^{-0.5} R(f) = N_{it}^{-0.5}[1 + (f/f_c)^2]^{-3}, \qquad \text{(A3)}$$

was fitted to the data of Fig. 3(C) at 0.5–30 Hz with the method of least squares. On the basis of equation (4), $Q(f)$ is equal to $[N_{tc}(f)P^2(f)]^{-0.5}$. The least squares fit was obtained by finding the minimum of

$$\begin{aligned} G &= \sum_{j=1}^{n} [(Q_j^{+1/3} - k_1' - k_2' f_j^2)/Q_j^{-1/3}]^2 \\ &= \sum_{j=1}^{n} (1 - k_1'/Q_j^{-1/3} - k_2' Q_j^{-1/3} f_j^2)^2. \end{aligned} \qquad \text{(A4)}$$

Equation (A4) is transformed to equation (A2) by substituting $x_{1j} = Q_j^{1/3}$ and $x_{2j} = Q_j^{1/3} f_j^2$. In equation (4a) $k_1' = N_{it}^{1/6}$ and $k_2' = N_{it}^{1/6} f_c^{-2}$. Hence, $N_{it}^{-0.5} = 1/k_1'^3$ and $f_c = (k_1'/k_2')^{1/2}$.

Goodness of fit

The goodness of the fit of a smooth curve to the data was estimated as follows. First we calculated the root mean square error of the experimental data (Y) from the predicted values (Y_{est}):

$$\epsilon_{rms} = \sqrt{1/n \sum_{j=1}^{n} (\log Y_j - \log Y_{jest})^2} \qquad \text{(A5)}$$

We used log Y instead of Y, because Y is plotted on a logarithmic scale. The values of Y_{est} were calculated by means of the relevant equation. The goodness of fit in percentages was then calculated as

$$GoF = 100(-k\epsilon), \qquad \text{(A6)}$$

where $k = 1$ for contrast sensitivity but 1/2 for η, N_c etc. as they are measures based on contrast squared. Thus, GoF is 85% if on the average log $(S/S_{est}) = \pm 0.15$ i.e., $S_{est} = \sqrt{2}S$ or $S/S/\sqrt{2}$. The value of GoF is the same if e.g. $\eta_{est} = 2\eta$ or $\eta/2$.